Disentangling human grasping type from the object's intrinsic properties using low-frequency EEG signals

Andreea I. Sburlea [a], Marilena Wilding [a], Gernot R. Müller-Putz [a, b, *]

[a] *Institute of Neural Engineering, Graz University of Technology, Graz, 8010, Stremayrgasse 16/4, Styria, Austria*
[b] *BioTechMed Graz, Austria*

ARTICLE INFO

ABSTRACT

Grasping movements are known to activate the fronto-parietal brain networks both in human and non-human primates. However, it is unclear if these activations represent properties of the objects or hand postures or both at different stages of the movement. We manipulated the intrinsic properties of the objects and the grasping types in order to create twelve unique combinations of grasping movements and we investigated, in healthy adult humans, the low-frequency time-domain EEG representation of grasping over different stages of the movement. Next, we implemented two multiclass decoders for the grasp type and objects' properties and evaluated them over time. Furthermore, we investigated the similarity between these grasping EEG representations and categorical models that encode properties of the movement and intrinsic properties of the objects. We found that properties of the grasping movement (grasp types, number of fingers) and intrinsic object properties (shape and size) as represented in EEG are encoded in different brain areas throughout the movement stages. Both object properties and grasp types can be decoded significantly above chance level using low-frequency EEG activity during the planning and execution of the movement. Moreover, we found that this preferential time-wise encoding allows the decoding of object properties already from the observation stage, while the grasp type can also be accurately decoded at the object release stage. These findings contribute to the understanding of the grasping representation based on noninvasive EEG brain signals, and its evolution over the course of movement in relation to categorical models that describe the grasped object's properties or that encode properties of the grasping movement. Moreover, our multiclass grasping decoders are informative for the design and implementation of noninvasive motor control strategies.

1. Introduction

Grasping seems an effortless and almost automatic movement. The shape and the size of an object play an important role in the way we grasp it. Upon distinguishing objects (Biederman, 1987), we can shape our hands according to their appearance in order to interact with them (Napier, 1956; Smeets and Brenner, 1999). Albeit we can perform reach-and-grasp movements with ease, their underlying neural mechanisms are highly complex and involve extensive computational resources (Fagg and Arbib, 1998; Castiello, 2005). When performing a grasping movement, our brain translates the visual representations of an object relative to its intrinsic properties such as shape, size, or weight, into multidimensional motor commands that inform different grasping types and hand configurations (Jeannerod et al., 1995). Therefore, grasping an object requires the integration of sensory, motor and visual

parameters. One of the brain networks that are involved in transforming visual features into motor commands is the fronto-parietal loop. To better understand the contribution of different brain regions during grasping, and potentially inform a more accurate control of a robotic limb, it is necessary to understand whether different brain regions encode grasping type, objects properties or both, at different stages of the grasping movement.

Several studies have investigated the neural patterns associated with grasping movements in non-human primates (Schaffelhofer and Scherberger, 2016; Castiello, 2005; Donoghue et al., 1998; Michaels and Scherberger, 2018) and in humans using different acquisition modalities: invasive, such as single-cell recordings (Klaes et al., 2015; Aflalo et al., 2015), local field potentials (LFPs) (Mollazadeh et al., 2008), electrocorticography (ECoG) (Jiang et al., 2020; Pistohl et al., 2012) and noninvasive, such as functional magnetic resonance imaging (fMRI)

(Cavina-Pratesi et al., 2007; Culham et al., 2003; Perini et al., 2020; Fabbri et al., 2016), functional near-infrared spectroscopy (fNIRS) (Koehler et al., 2012; Wriessnegger et al., 2017), positron emission tomography (PET) (Rizzolatti et al., 1996; Grafton et al., 1996), magnetoencephalography (MEG) (Buch et al., 2012; Taniguchi et al., 2000) and electroencephalography (EEG) (Sburlea and Müller-Putz, 2018; Guo et al., 2019; Iturrate et al., 2018; Koester et al., 2016; Sburlea AI, Müller-Putz GR, 2019).

Building upon these findings it becomes relevant to gain a good understanding of the neural correlates of grasping at different stages of the gradual unfolding of the movement. Non-invasive acquisition modalities, such as EEG, provide high temporal resolution of neural activity over large brain regions, making it an appealing technique to study the changes of brain patterns associated with the grasping movement over time. In addition to the fundamental understanding of the underlying mechanisms of grasping movements, several studies have focussed on the prediction and classification of grasping movements at the single-trial level for the control of a brain-computer interface or an upper-limb neuroprosthesis using movement-related cortical potentials (MRCPs) (Schwarz et al., 2018; Iturrate et al., 2018; Omedes et al., 2018; Hazrati and Erfanian, 2010; Zaepffel et al., 2013; Jochumsen et al., 2016; Agashe et al., 2015; Ofner, 2019; Muller-Putz et al., 2019).

In this study, we aim to gain a better understanding of the neural mechanisms underlying grasping, as encoded by low-frequency EEG amplitudes, and potentially inform future BCIs about the features that can lead to a good discriminability among objects and among grasp types at different movement stages. We set three research goals. First, we will evaluate the performance to classify grasping movements at different stages of the movement using non-invasive low-frequency time-domain EEG measures of brain activity. Next, we will investigate whether object properties and/or grasp types are encoded at these stages. And, third, we will study the representation of these grasping characteristics and how they drive classification. We hypothesize that during the planning and execution stage the decoding performance would be higher than at rest stages and that the grasping representation from motor related brain areas would drive the performance. Furthermore, we surmise that object properties would be represented in the EEG channel space covering visual related brain areas earlier in the unfolding of the grasping movement, while the grasp type and the number of fingers used in the grip would be represented later in the progress of the movement by the channels covering brain areas targeted by planning and motor processes. To address these questions, we designed a study that allowed us to separate between object properties and grasp types. Participants observed, grasped, held and released objects of 2 different sizes and 2 different shapes using 3 different grips. We used a multiclass classification approach to distinguish among grasp types and among objects based on their intrinsic properties. Next, we performed representational similarity analysis in order to further understand the relationship between the EEG representation of grasping (from the perspective of grasp type, number of fingers involved and object properties) and categorical models that encode these characteristics of grasping. With this analysis, we gained insights about the interplay of distinct brain networks during the course of grasping movements, as well as about the representational space in which alike grasping movements are encoded, using noninvasive EEG signals.

2. Materials and methods

2.1. Participants

We recruited 16 healthy right-handed participants between the age of 20–32 years (9 females, mean age = 25.3 years, SD = 3.5 years) who were free of neurological diseases and had a normal or corrected-to-normal vision. The extent of hand-lateralization/dominance was examined with an adapted version of the Edinburgh Handedness Inventory (Oldfield, 1971), which assesses the preferably used hand for

several grasping types. The study was conducted in accordance with the Declaration of Helsinki (1975) and it was approved by the local ethics committee of the Medical University of Graz. After a standardized instruction, the participants signed the informed consent form. The participation was honored with 7.50€ per hour.

2.2. Experimental paradigm

Participants underwent a short practice session in order to familiarize themselves with the task paradigm, which was implemented in the MATLAB-based Psychtoolbox (version 3). After the familiarization phase, the main experiment started. The participants were seated in front of a computer screen which showed the paradigm of the experiment. The task was to replicate the shown grasping as closely as possible, using their right hand and the respective object, which was centrally placed between the screen and the participant. In the first 3 s of the trial (fixation phase), participants were instructed to fixate their gaze on a cross located in the middle of the screen and to avoid eye movements. Next, in the observation phase, an image of the grasping movement involving the object (lying on the table in front of the participant) was shown on the screen for 4 s. During this phase, participants were instructed to observe the grasping posture as well as the shape and size of the shown object. In the following execution phase, the previously observed movement should be executed after an 'x' symbol appeared on the screen. Before the movement execution, participants were asked to focus their gaze on the object and keep it there until the end of the movement. Participants could execute the movement within 4 s and were instructed to hold it until the "Relax" instruction appeared on the screen. In the last phase (relaxation phase), the "Relax" -instruction appeared for 2 s, followed by the instruction "Get ready.", marking the preparation time for the next trial. During the observation and relaxation phase, participants were not restricted in their eye movements. During the fixation, observation, and relaxation phase, the right hand was placed on a resting position on a black mousepad, which facilitated the recording of resting muscle and joint tracking activity.

The experiment consisted of 24 runs (of approximately 7 minutes each) in which participants were asked to perform three different types of grasp: power, five-finger precision, two-finger precision, in a random order using one of the four different objects: large cylinder (diameter = 5 cm, length = 24 cm), small cylinder (diameter = 3 cm, length = 24 cm), large sphere (radius = 8 cm) and small sphere (radius = 5 cm) (see Fig. 1). All the objects were made of wood and had the same texture. They were manually painted with the same color. The images of grasping movements were taken with a professional Nikon D3500 camera, located on a fixed tripod to ensure the same characteristics of the images. Each run contained 27 trials and the object that was grasped remained the same for the entire run. Each trial lasted 15 s, resulting in a total measuring time of approximately 3 h. In total, each of the 12 grasping conditions was executed 54 times. After every run, the participants had the opportunity to take a small break.

2.3. Data acquisition

EEG data was recorded using a 64-EEG channel ActiCap system connected to two 32-channel BrainAmp amplifiers (BrainProducts, Germany). Brain activity was measured by 61 channels, which covered all brain regions, according to the 10-10 international system. EOG activity was measured with three electrodes mounted on the outer canthi of the left and right eyes and above the nasion. The ground electrode was placed on AFz and the reference electrode was attached to the left mastoid.

In order to track the participants' movements as well as to determine their exact kinematics, we used an optical tracking device (Leap Motion Inc., San Francisco, CA, USA). Additionally, muscle activity (EMG) was recorded with a bracelet of eight equidistant EMG sensors (Myo bracelet, Thalmic Labs Inc., Ontario Canada), which was mounted on the right
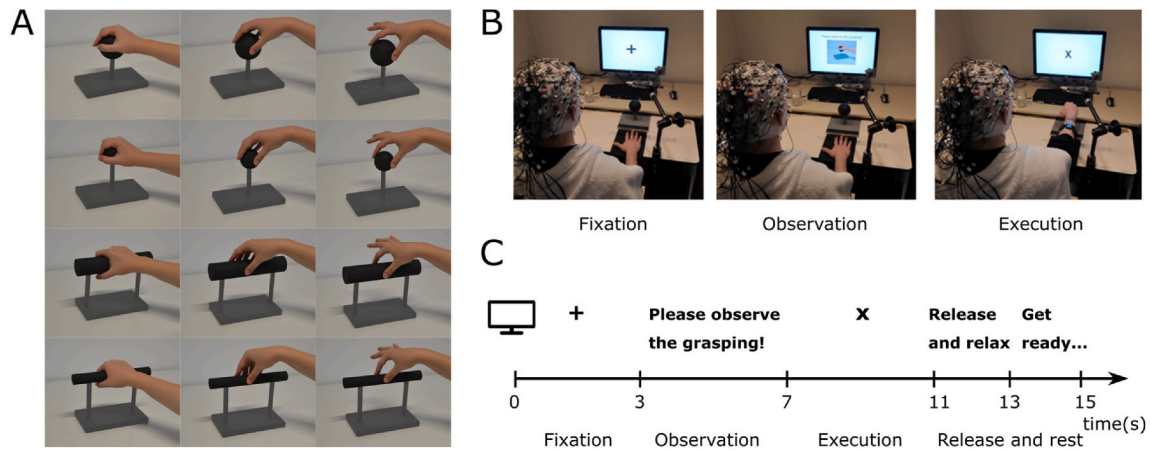
Fig. 1. (A). Display of the four different objects (rows: large sphere, small sphere, large cylinder, small cylinder) and the three different grasping types (columns: power, five-finger precision, two-finger precision), resulting in 12 different conditions; (B). Pictures of a participant in different stages of the experiment; (C). Timeline of a trial and presentation cues.

arm (below the elbow), above the extrinsic hand muscles. Before use, an individual calibration of the bracelet, which is connected via Bluetooth, was necessary. These behavioral data were recorded for the investigation purposes of another study. The Lab Streaming Layer (LSL) (htt ps://github.com/sccn/labstreaminglayer) was utilized to enable simultaneous acquisition of the different data streams. In addition, a photodiode was used to align the data to the visual presentation of the stimuli on the monitor.

2.4. Data preprocessing

Data was preprocessed in Matlab R2016b. As a first step, the data was filtered, using a Butterworth fourth-order, zero-phase, band-pass filter between 0.1 and 40 Hz and then downsampled to 100 Hz. From a total of 648 trials, on average 4 trials were missing per participant due to absent markers during the recording. Next, we performed an independent component analysis (ICA) over all four objects in order to extract maximally independent components, which represent synchronous activity within certain cortical areas and thereby exclude artifactual components. To further eliminate artifacts in the functional data, we applied SASICA (Semi-Automatic selection of Independent Component Analysis) (Chaumon et al., 2015), which automatically marks artifactual components for rejection (which correspond to muscle or eye movements), based on several selection algorithms. Both tools are implemented in the EEGLAB toolbox. The single components were then visually inspected for definite rejection. After that, the single runs were again filtered by making use of a Butterworth fourth-order, zero-phase, band-pass filter from 0.1 to 3 Hz, and MRCPs were computed for 61 EEG channels. We removed the first second from the fixation period due to artifact contamination coming from the break period. Therefore, we define the beginning of the trial as the second one of the fixation period and we will refer to it as the "0" point. Next, we split the trial into stages of the movement: the fixation stage starts from the "0" point until second 2; the observation stage is between second 2 and second 5; the planning and execution stage is between second 5 and second 8; the holding stage is between second 8 and second 10; the releasing stage is between second 10 and second 12.

2.5. Multi-class classification analysis

We designed two multiclass classifiers in order to discriminate between grasp types: power, precision with five fingers and precision with two fingers, and between intrinsic properties of the objects: large cylinder, small cylinder, large sphere and small sphere. We examined the performance of these classifiers in the five stages of the movement:

fixation, observation, planning and execution, holding and releasing.

Both classifiers were based on regularized linear discriminant analysis (LDA) and were using low-frequency amplitude (time-domain) features of the 61 channels from the respective time windows. From the band-pass filtered data between 0.1 and 3 Hz, we extracted one feature every 250 ms. We assumed that all our classes have the same covariance structure, hence we fitted a multiclass linear model. We used regularization and 10*10 fold cross-validation for training and testing. We chose within class accuracy as our metric of performance, and we computed it as the percentage of correctly classified trials for that class taken from the total number of trials of that class. We also evaluated the discrimination among grasp types and among objects during the movement progression, independent of the movement stages, in order to better understand the dynamics of the process. We evaluated every 50 ms the discrimination accuracy of the multiclass decoder. We included this analysis in the Supplementary Material Fig. S3.

To get an overall understanding of the behavior of these two classifiers (for grasp type and for object properties) across the stages of the movement, we also computed accuracy as the percentage of correctly classified trials from the total number of trials independent of the class. To examine the statistical significance of our results we used pairwise Student t-test evaluation and corrected our p-values by accounting for multiple comparisons using the Bonferroni-Holm correction (Holm, 1980).

2.6. Similarity analysis

To assess the extent to which different brain regions encode different attributes of the grasping movement, we performed a representational similarity analysis (Kriegeskorte et al., 2008). For each of the five stages (temporal windows), we conducted a searchlight analysis (Su et al., 2012; Sburlea and Müller-Putz, 2018) over the channel space. Specifically, from the average EEG pattern over the trials of each of the twelve conditions, we extracted standardized (z-scored) EEG amplitude patterns at different spatial locations. For the analysis, we defined 31 neighborhoods (regions of interest) in the channel space. One neighborhood had five members: one centroid and four equidistant neighbors, and had 2 members in common with another neighborhood. All the information within one neighborhood was concatenated into a vector. This vector defined the pattern of activity for the region with a given centroid in the channel space. We computed the EEG reference representations based on the searchlight analysis of the time-domain EEG data in the five movement stages: fixation, observation, planning and execution, holding, and release. The searchlight analysis yielded a total of 31 reference representation dissimilarity matrices (RDMs)

([Kriegeskorte et al., 2008](#)) with dimension 12 × 12 (condition x condition) for each movement stage.

We used 1-r (where r is the Pearson correlation) as the distance metric between the patterns of different conditions. Next, we ranked and scaled the distances between 0 and 1, and computed the RDMs between pairs of grasping conditions. Specifically, to construct the reference RDMs we compared the normalized neural patterns of activity of the different grasping conditions, extracted previously for each movement stage. Then we computed categorical models for three categories: grasp type, object properties and number of fingers. The RDMs of these categorical models were binary representations, which contained a 0 for each pair of stimuli falling into the same category and a 1 for each pair of stimuli falling into different categories.

To visualize the distances between the representations of different grasping movements, we used multidimensional scaling (MDS) ([Kruskal and Wish, 1978](#)). MDS is a general dimensionality reduction method that projects entities in a low-dimensional space, such that their distances reflect their similarities. Specifically, similar entries will be located closer to one another, while dissimilar ones will be farther apart. For MDS visualization as a 2D plot, we used the Matlab function mdscale, which performs nonmetric MDS for two dimensions with the squared stress criterion. To examine the statistical significance of our results we used Kendall's Tau b correlation coefficient to assess the similarity between the EEG representations and the categorical models and corrected the associated p-values by accounting for multiple

comparisons using the Bonferroni-Holm correction ([Holm, 1980](#)).

3. Results

3.1. Behavioral analysis

The median reaction time from the execution cue, across conditions and subjects, was 535 ms and the 25th to 75th percentile range was [430, 675] ms. We present the reaction times of every trial for all subjects and conditions in the Supplementary Material Fig. S1. We performed a Wilcoxon ranksum test to evaluate if the reaction times were consistent among conditions and we found no statistically significant difference (alpha = 0.05), which indicates that subjects had a similar reaction time in all the conditions.

The duration of the movement was consistent across conditions and subjects and its median was 1.44 s and the 25th to 75th percentile range was [1.40, 1.47] s. We present the duration of the movement for every condition and subject in the Supplementary Material Fig. S2. We performed a Wilcoxon ranksum test to evaluate if the duration of the movement was consistent among conditions and we found no statistically significant difference (alpha = 0.05), which indicates that subjects performed the grasping movement in every condition with the same time length.
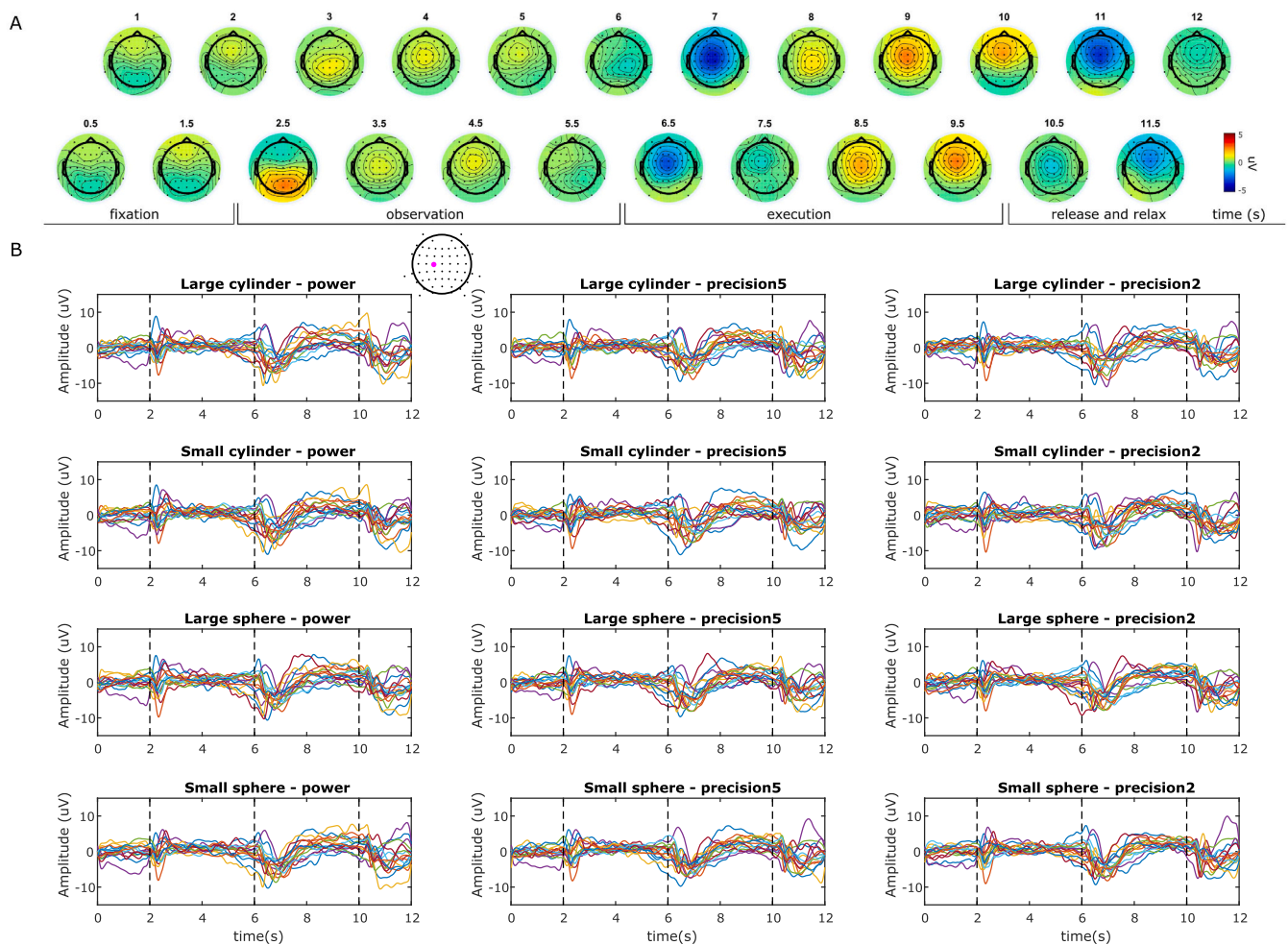

Fig. 2. Neurophysiological results. (A). Grand average topoplots showing the low-frequency amplitude content for the average of all grasping conditions. Vertical dashed lines indicate the cues of the paradigm (at second 2: image observation, at second 6: movement execution, and at second 10: release and relax). (B). MRCP traces for each of the 12 grasping conditions in channel C1 marked with a magenta dot (top of the panel). Individual traces correspond to subjects.

3.2. Neurophysiology

Fig. 2 presents the unfolding of the neural correlates of grasping in the low-frequency amplitude across different stages of the movement. In Fig. 2A, we show the grand average patterns of all conditions and we observe around second 6 a slight negativity in the parietal areas. This negativity pattern becomes more pronounced towards second 7, which coincides with the initiation of the movement. This pattern is known as the movement-related cortical potential (MRCP), and it is associated with the planning and execution of the movement. It appears on the contralateral side over fronto-central, central and parietal regions. A similar pattern can be observed during the release stage around second 11 when another movement is planned and executed. Fig. 2B shows, for channel C1, the average MRCP traces of each subject for every grasping condition.

3.3. Multi-class classification

Fig. 3 presents the multi-class classification results for grasp type (A) and for object properties (B). We found higher classification results for the precision two fingers type of grasp than for the other two types throughout all the stages but the fixation, at which all the results were at chance level (33%). The power grasp was better classified than the precision five fingers type in all the stages of the grasping.

The classification based on the object intrinsic properties showed the highest within-class accuracy during the planning and execution stage. The accuracies were comparable also in the release stage. During the observation stage we could discriminate well objects based on their shape, but not on their size. At the fixation and holding stages, the accuracy was around chance level (25%).

Fig. 4 summarizes the classification results by removing the class specificity and reporting the results for the two classification approaches and over the grasping stages. As anticipated from Fig. 3, for the classification of grasp type, during the planning and executing stage, as well as during the release stage we reached the highest accuracy. Moreover, the obtained accuracy was significantly higher than during the fixation and holding phases when the movement was absent and minimized,

respectively. During the observation stage, the accuracy was significantly larger than during the fixation stage, but not significantly different than during the holding stage. The high accuracy obtained at the release stage suggests that the categorization of release movements is highly related to grasp types.

Regarding the classification of objects, we obtained the highest accuracy during the planning and execution and during the observation stages. Moreover, the accuracy in the two stages was not statistically different, indicating the possibility to correctly predict the object to be grasped from the EEG features before the movement execution. Interestingly, during the fixation stage when subjects were already presented with the object that they would have to grasp later on, their accuracy was only slightly above chance level. Hence, the classification of the object in the context of grasping is not only driven by visual information but also by the motor command (grasp type) presented during the observation stage when the accuracy was significantly higher. During the release stage, we obtained significantly higher accuracy than during the fixation and holding stages, indicating once again the relevance of the movement information and only the visual processing for the classification of the objects in the context of grasping.

3.4. Representational similarity analysis

Next, in order to get more insights about the representation of the features that drive the accuracy, we conducted the representational similarity analysis between the EEG reference representations and three categorical models that encode grasp type, number of fingers used for grasping and object properties. Hence, in Fig. 5A we present the three categorical models as binary models, in which a distance equal to 0 indicates belonging to the same category and a distance equal to 1 indicates belonging to another category. Fig. 5B shows the distribution of the representation similarity over fronto-central, central, centro-parietal and parietal brain areas between the EEG representational dissimilarity matrices and the three categorical models.

During the fixation stage, the largest similarity (smallest distance) is observed over parietal areas on the ipsilateral side for the comparison with the model that encodes object properties (bottom row); while grasp
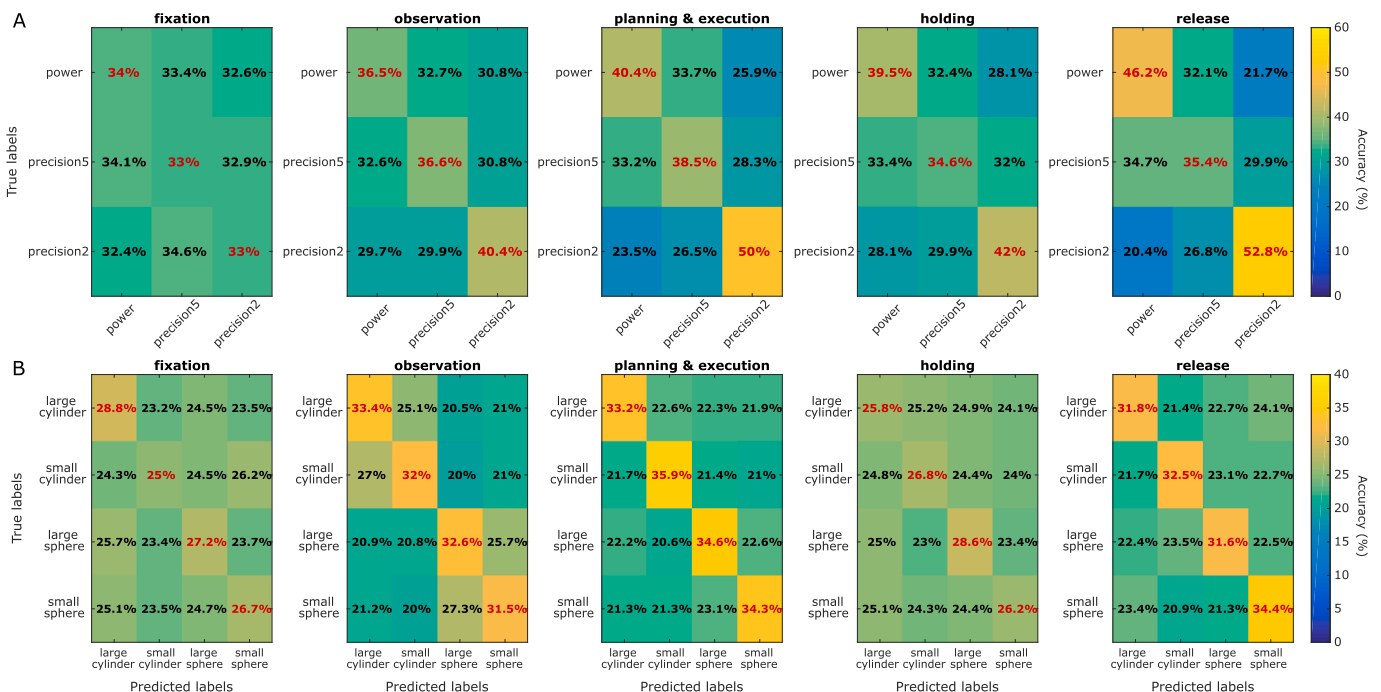

Fig. 3. Multi-class classification according to grasp type (A) and object properties (B) at different stages of the movement: fixation, observation, planning and execution, holding, and release.
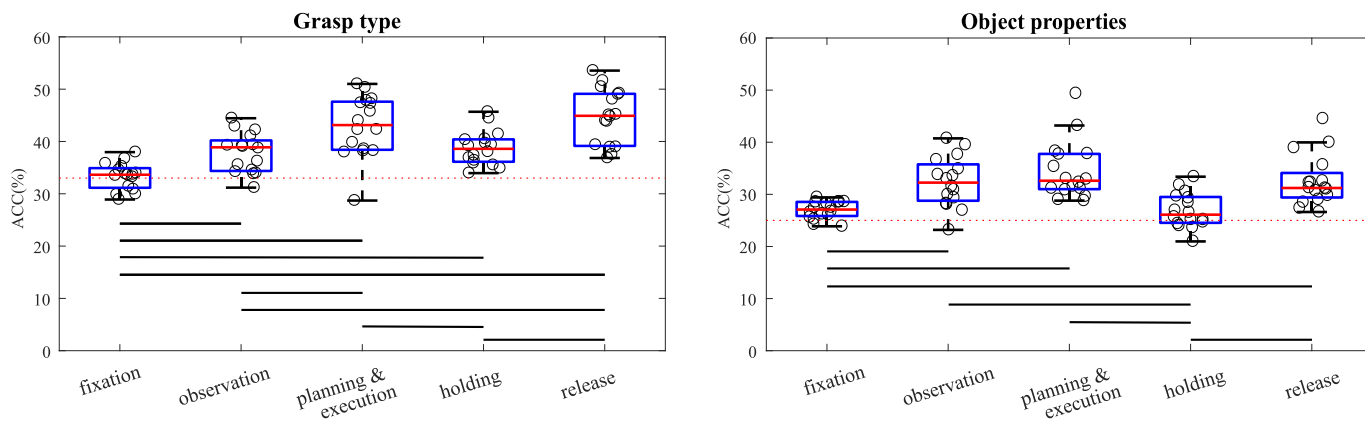
Fig. 4. Accuracy as a percentage of correctly classified trials from the total number of trials independent of the class, at different stages of the movement for the two classifiers based on grasp types: power, precision with five fingers and precision with two fingers (on the left) and on intrinsic properties of the object: large cylinder, small cylinder, large sphere, small sphere (on the right). The stars indicate the level of statistical significance (*$p < 0.05$, **$p < 0.01$, ***$p < 0.001$, ****$p < 0.0001$). The dotted line marks the chance level of each classifier. Regarding the boxplots, we show the median with a red line, and the bottom and top edges mark the 25th and the 75th percentiles, while the whiskers cover the entire range of the data excluding the points that are considered outliers.
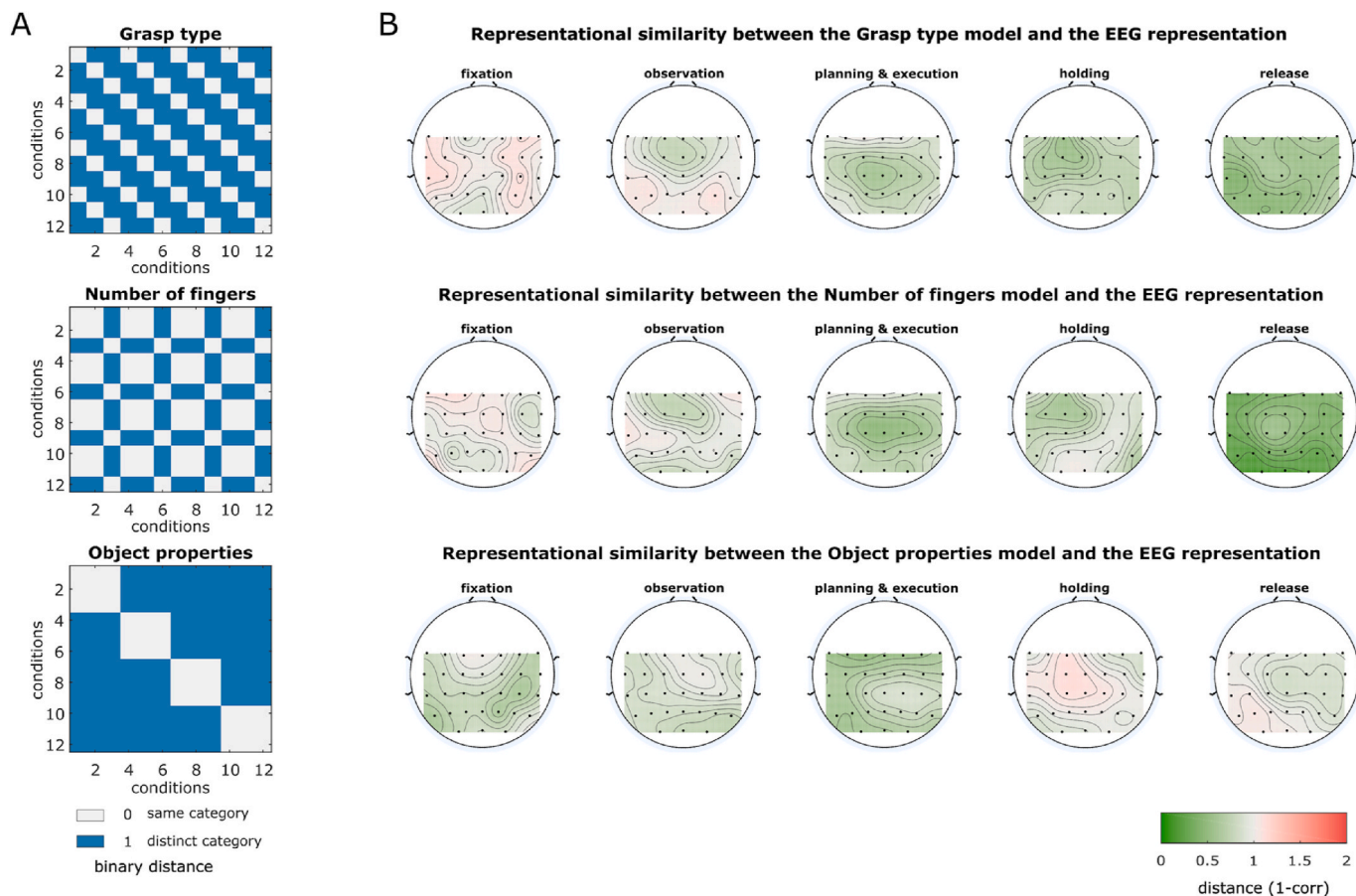

Fig. 5. Representational similarity analysis. (A). Categorical models describing grasp type (top), number of fingers (middle) and object properties (bottom). The 12 conditions are ordered as follows: 1. large cylinder power, 2. large cylinder precision5, 3. large cylinder precision2, 4. small cylinder power, 5. small cylinder precision5, 6. small cylinder precision2, 7. large sphere power, 8. large sphere precision5, 9. large sphere precision2, 10. small sphere power, 11. small sphere precision5, 12. small sphere precision2. (B). RSA patterns between the standardized low-frequency amplitude EEG and the three categorical models from A across the five stages of the grasping movement. The 31 dots overlapping the RSA pattern mark the centroids of the regions of interest used in the searchlight analysis.

type and number of fingers were not presented at this stage and therefore not represented in the EEG representations. At the observation stage, the grasp type (top row) and number of fingers (middle row) are very well represented over contralateral fronto-central and central areas, while object properties appear encoded in parietal areas. Next, at

the planning and execution stage, the grasp type and number of fingers show similar representations over the central and centro-parietal areas related to motor processing; while object properties appear represented in the fronto-central and parietal areas. At the holding stage, only the grasp type and the number of fingers show similarities with the EEG

patterns. These similarities are represented on the contralateral side at fronto-central and central areas. Finally, at the release stage, the grasp type and the number of fingers are more strongly represented than the object properties. The representation similarity with the first two categorical models appears over centro-parietal and parietal areas; while objects are represented ipsilaterally over central and centro-parietal areas.

For the next analysis, we focused on the planning and execution stage. Specifically, in Fig. 6A we use multidimensional scaling to describe the relationship between the twelve grasping conditions over six brain regions. These six regions are depicted with dotted circles in Fig. 6A. Each region contains five channels and we specify the label of the centroid of each region. The lines that connect the grasp pictograms correspond to the four objects: large cylinder (red), small cylinder (green), large sphere (blue), small sphere (yellow).

In Fig. 6B we quantify the similarity between the EEG representations of grasping conditions over each of the six brain regions and the three categorical models, during the planning and execution stage using Kendall' Tau b which ranges between −1 (negative association) and 1 (positive association), with 0 indicating the absence of association, and we report the associated p-values corrected for multiple comparisons. We found that grasp type and number of fingers are more strongly represented over central (rho = 0.26, p = 0.01; rho = 0.35, p = 0.002, respectively) and parietal areas (rho = 0.27, p = 0.015; rho = 0.39, p = 0.001); while object properties are strongly represented over frontro-central (rho = 0.42, p = 0.0001) as well as over parietal areas (rho = 0.25, p = 0.01).

4. Discussion

We found that properties of the grasping movement (grasp types, number of fingers) and intrinsic object properties (shape and size) are represented in the low-frequency time-domain EEG activity of different brain areas throughout the movement stages. Both object properties and
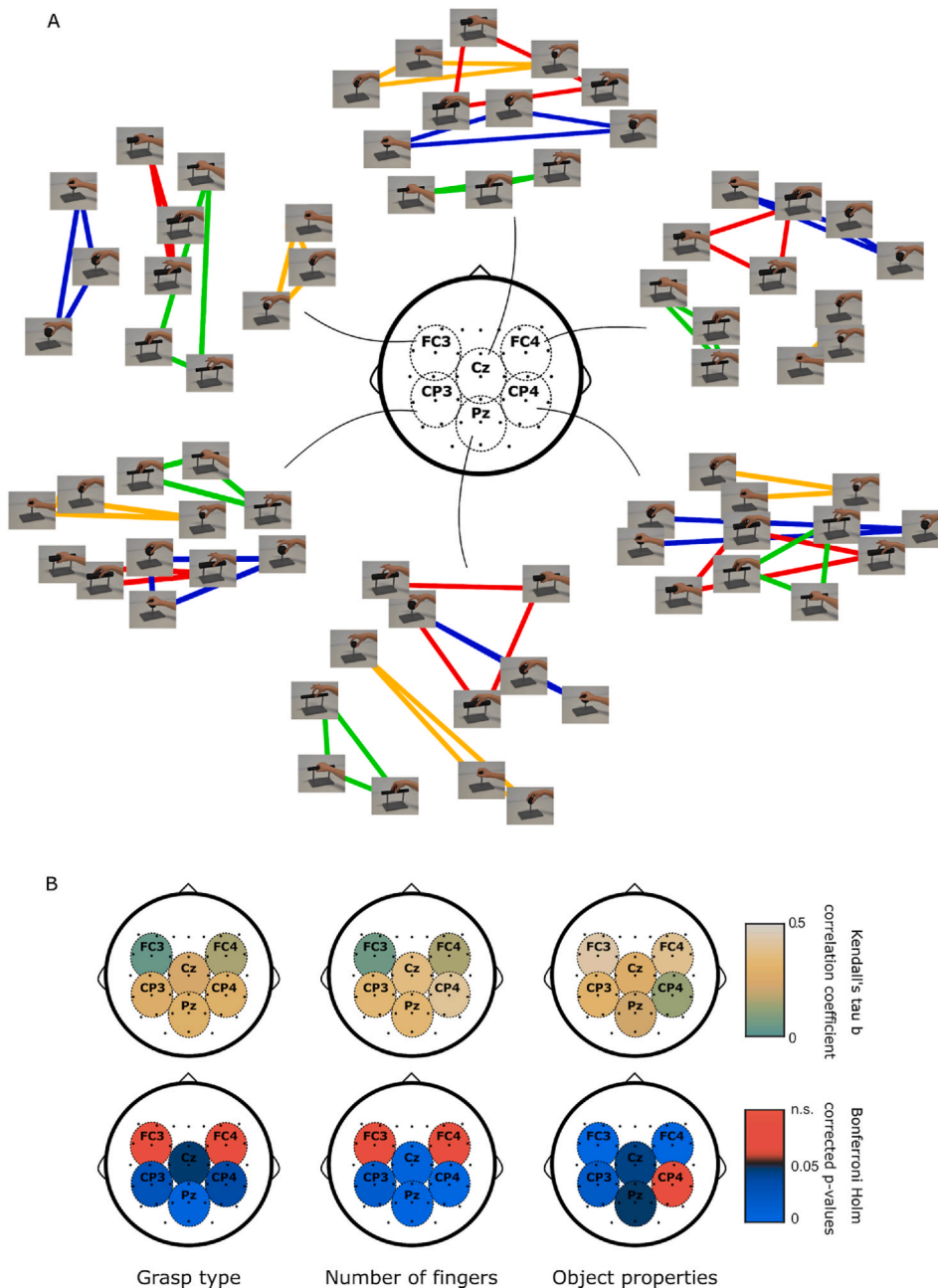

Fig. 6. A. Multidimensional scaling of grasping conditions at six brain regions during the planning and execution stage of the movement. The color of the lines connecting the pictograms correspond to the four objects: large cylinder (red), small cylinder (green), large sphere (blue) and small sphere (yellow). B. Statistical assessment of similarity during the planning and execution stage of movement over the six brain regions presented earlier. Kendall's tau b correlation coefficient (top row) and the associated Bonferroni-Holm corrected p-values between the EEG RDMs of the six regions and the three categorical RDMs that capture grasp type, number of fingers and object properties.

grasp types can be decoded significantly above chance level during the planning and execution of the movement. Moreover, we found that this preferential time-wise representation allows the decoding of object properties already from the observation stage, while the grasp type can also be accurately decoded at the planning and execution stage and at the object release stage.

To disentangle the properties of objects from types of grasps over the course of the movement, we designed twelve conditions in which we combined three grasp types with four objects. These combinations allowed us to later group the conditions according to the two factors (i. e., grasp type and object properties). Next, we trained and tested two multi-class classifiers on data, independent of the type of grasp and object properties, respectively. Moreover, we used representational similarity analysis to inspect the EEG representations of grasping during the course of the movement in relation to three categorical models that encode types of grasp, numbers of fingers involved in grasping, and properties of the objects.

Grasping involves the processing of the object's intrinsic properties such as shape and size, and the transformation of these properties into a hand configuration resulting in a type of grasping movement (Jeannerod et al., 1995; Turella and Lingnau, 2014). Reaching and grasping movements have been described by the interaction between perceptual and motor systems, through the communication between dorsal and ventral streams (van Polanen and Davare, 2015).

In monkeys, the inferior parietal lobule and the inferior premotor area (area F5) have been shown to participate in the transformation of an object's intrinsic properties into specific grasp types (Murata et al., 2000; Rizzolatti and Fadiga, 1998; Michaels and Scherberger, 2018). Both areas have been found to contain neurons that encode not only the shape, size, and orientation of objects, but also specific types of grasping postures necessary to grasp them. Studies on humans with lesions to the parietal lobe confirm that object's intrinsic properties relevant for grasping are processed by the parietal lobe, and also demonstrate the dissociation between the visual processing of objects ("pragmatic" analysis) and the meaning of the grasp type related with the context of the movement ("semantic" analysis) performed by the temporal lobe (Binkofski et al., 1998; Jeannerod et al., 1995).

The fronto-parietal network relates the visual processing of the object properties with the spatial configuration of the fingers into a suitable type of grasping, by exchanging information through the ventral and dorsal route. When one of these routes is disturbed or interrupted due to optic ataxia, lesions to the occipito-temporal lobe or parietal lobe, either the discrimination of the objects or the correct grasp type configuration is compromised (Goodale et al., 1991; Jeannerod et al., 1994). Grasping movements have been also investigated in other patients with different motor disabilities such as paraplegia or tetraplegia (Bockbrader, 2019; Ajiboye et al., 2017; Rastogi et al., 2020; Muller-Putz et al., 2019; Ofner et al., 2019).

In terms of neurophysiology, in the current study, we found the MRCP to occur in contralateral central and centro-parietal regions during the planning and execution stage of grasping and to be more centrally localized during the release stage. Previous studies investigating goal-directed grasping movements in humans using EEG have shown MRCP patterns with similar representations in terms of amplitude and localization. Specifically, we reported in a previous study (Schwarz et al., 2018) involving cue-based palmar, pincer and intermediate grasping movements that the associated MRCP patterns were found over central and parietal brain areas. Other EEG patterns associated with grasping movements have been reported by (Iturrate et al., 2018), in which they investigated power and precision grasps with a focus on broadband rhythms, in particular, the alpha frequency band and its associated connectivity between the different brain areas involved in grasping. The beta frequency band has also been shown by (Zaepffel et al., 2013) to carry information about the prior knowledge of grip and force parameters upon the planning and execution stages of grasping movements. In a recent paper (Guo et al., 2019), the authors

have shown for precision grasps that the visual properties of the object and the orientation of the grasping, as represented in EEG, have different representations during the planning and execution of the movement. In previous studies (Sburlea and Müller-Putz, 2018; Sburlea AI, Müller-Putz GR, 2019), we investigated in healthy subjects the relation among a large variety of grasping movements in terms of their neural and behavioral representations in different stages of the movement. We found that the shape and size of the grasped object are encoded in the higher frequency EEG representation during the hand-preshaping stage; however, the encoding of these object properties, as well as the type of grasp in the low-frequency EEG, remained unclear.

In a recent study (Fabbri et al., 2016), looked into the representation of object properties and grasp types using fMRI and found that object elongation is the most strongly represented object feature during grasping and is coded preferentially in the primary visual cortex as well as the anterior and posterior superior-parieto-occipital cortex. By contrast, primary somatosensory, motor, and ventral premotor cortices coded preferentially the number of digits while ventral-stream and dorsal-stream regions coded a mix of visual and motor dimensions. Moreover, the difference between the number of fingers involved in the grasping movement has been shown to be specifically encoded in the ventral premotor cortex (Cavina-Pratesi et al., 2018). Indeed, our current findings using low-frequency time-domain EEG activity indicate that at the planning and execution stage, the channels covering fronto-central and parieto-occipital brain regions are involved in processing object's properties, while the channels covering the primary somatosensory, motor and parietal brain regions are recruited for the processing of grasp types and number of fingers used for grasping.

In terms of classification, we obtained significantly higher performance for the classification of grasp types during the planning and execution stages, and release stages compared to the other stages; while the classification of objects was already significantly higher than the chance level during the observation stage. On a finer time scale, we found a high discriminability between objects in the first 300 ms of the observation stage, associated with the visual representation of the objects in occipital areas. Objects could be separated with consistent performance throughout the entire planning and execution stage, while grasp types reached peak performance after the movement cue. Our findings are comparable with the performance reported earlier (Schwarz et al., 2018); however, different types of grasping movements have been previously evaluated.

The observation stage, which can also be seen as a delay period of the grasping movement, has been shown to improve the visuomotor performance, by involving networks associated with object memorization which are arguably independent of the posterior parietal cortex associated with the grasping movement (Himmelbach and Karnath, 2005; Sburlea and Müller-Putz, 2018; Sburlea AI, Müller-Putz GR, 2019). The relevance of the delay period has been highlighted by the case of patients with optic ataxia, which consisted of severe bilateral damage to the homolog of the monkey's "dorsal stream" of visual processing, causing visuomotor difficulties (Milner et al., 2001; Blangero et al., 2008). Their findings indicate that vision can guide action through alternative networks than the ones involving the parietal lobe. The recruitment of these alternative networks helped the patient's grasping difficulties, at the cost of taking more time to process vision into action. In our study, we also observed a different representation of object properties and grasping types during the observation stage. Indeed, parietal activations were present in the representation of object properties, while motor and sensorimotor areas described the grasp types as well as the number of fingers necessary for the grasping movement. The interplay between visual inputs and motor intentions has been also reported by (Hebart et al., 2012) as the information exchange between visual cortex and inferior parietal cortex as a function of sensory evidence (Schone and Hunter, 2021).

A potential limitation in our study is the level of force involved in different grasping movements. Very recently, an intracortical BCI study

(Rastogi et al., 2020) in humans with tetraplegia, showed that force could be decoded in multiple grasp types. Nevertheless, authors have shown that grasp type was classified more accurately and had greater population-level representation than force. Therefore, decoding force information becomes even more meaningful when the decoder can reliably capture the grasp type information. Indeed, in our study we have not measured force levels because the task did not involve lifting or transportation of the objects; however, we observed high discrimination between grasp types also considering the number of fingers involved, which indicates that force does not play a pivotal role in the grasping movements presented in this study.

One relevant aspect of grasping is the context of the movement. Objects for daily life use are grasped according to the action to be performed (e.g., using the knife to cut a slice of bread requires a different grip than using the knife to spread the butter on the slice of bread). Recent studies have shown that visual and haptic inputs play an important role in skilled grasping (van Polanen and Davare, 2015; Camponogara and Volcic, 2019) and can influence the behavior of the movement in different phases, with haptics being more crucial in the initial phases and vision being more important for the final on-line control. Moreover, another recent study (Jarque-Bou et al., 2019) illustrated from a behavioral perspective using muscle and kinematic recordings of hand movements, the grasping interaction with daily life objects in one of the largest available datasets on goal-driven actions. Therefore, grasping objects for a daily living adds context to movement and should be considered in future studies.

To summarize, in this study we have shown that the information about grasp types and object properties encoded in the low-frequency time-domain EEG is not represented in isolation just by the channels over one brain region across the stages of grasping movement, but that channels covering different brain regions process these two types of information at several stages of the movement. Hence, we concluded that grasp types and object properties can be successfully decoded above chance level not only at the planning and execution stage of the movement but also at the observation (object properties) and the release (grasp type) stages. These findings are relevant for the implementation of future systems that study the control of grasping movements. In the future, we plan to evaluate such decoders also in individuals with spinal cord injury or in stroke end-users.

CRediT authorship contribution statement

Andreea I. Sburlea: Design of the experimental study, Data acquisition, Formal analysis, Writing - original draft, review & editing. **Marilena Wilding:** Data acquisition, Writing - review & editing. **Gernot R. Müller-Putz:** Design of the experimental study, Writing - review & editing.

Declaration of competing interest

The authors declare that they have no known competing financial interests or personal relationships that could have appeared to influence the work reported in this paper.

Acknowledgments

Appendix A. Supplementary data

Supplementary data to this article can be found online at https://doi.org/10.1016/j.ynirp.2021.100012.

References

Aflalo, Tyson, Spencer, Kellis, Klaes, Christian, Lee, Brian, Shi, Ying, Pejsa, Kelsie, Shanfield, Kathleen, et al., 2015. Neurophysiology. Decoding motor imagery from the posterior parietal cortex of a tetraplegic human. Science 348 (6237), 906–910.

Agashe, Harshavardhan A., Paek, Andrew Y., Zhang, Yuhang, Contreras-Vidal, José L., 2015. Global cortical activity predicts shape of hand during grasping. Front. Neurosci. 9 (April), 121.

Ajiboye, A. Bolu, Ajiboye, A. Bolu, Willett, Francis R., Young, Daniel R., Memberg, William D., Brian, A. Murphy, Miller, Jonathan P., et al., 2017. Restoration of reaching and grasping movements through brain-controlled muscle stimulation in a person with tetraplegia: a proof-of-concept demonstration. Lancet. https://doi.org/10.1016/s0140-6736(17)30601-3.

Biederman, Irving, 1987. Recognition-by-Components: a theory of human image understanding. Psychol. Rev. https://doi.org/10.1037/0033-295x.94.2.115.

Binkofski, F., Dohle, C., Posse, S., Stephan, K.M., Hefter, H., Seitz, R.J., Freund, H.J., 1998. Human anterior intraparietal area subserves prehension: a combined lesion and functional mri activation study. Neurology 50 (5), 1253–1259.

Blangero, Annabelle, Coello, Yann, Striemer, Chris, Rossetti, Yves, Danckert, James, Pisella, Laure, 2008. Dorsal and ventral stream interactions: evidence from optic ataxia. Brain and Cognition. https://doi.org/10.1016/j.bandc.2008.02.009.

Bockbrader, Marcia, 2019. "Upper limb sensorimotor restoration through brain–computer interface Technology in tetraparesis. Current Opinion in Biomedical Engineering. https://doi.org/10.1016/j.cobme.2019.09.002.

Buch, Ethan R., , Amirali Modir Shanechi, Fourkas, Alissa D., Weber, Cornelia, Birbaumer, Niels, Cohen, Leonardo G., 2012. Parietofrontal integrity determines neural modulation associated with grasping imagery after stroke. Brain: J. Neurol. 135 (Pt 2), 596–614.

Camponogara, Ivan, Volcic, Robert, 2019. Grasping movements toward seen and handheld objects. Sci. Rep. https://doi.org/10.1038/s41598-018-38277-w.

Castiello, Umberto, 2005. The neuroscience of grasping. Nat. Rev. Neurosci. 6 (9), 726–736.

Cavina-Pratesi, Cristiana, Connolly, Jason D., Monaco, Simona, Figley, Teresa D., David Milner, A., Schenk, Thomas, Culham, Jody C., 2018. "Human neuroimaging reveals the subcomponents of grasping, reaching and pointing actions." cortex. a Journal Devoted to the Study of the Nervous System and Behavior 98 (January), 128–148.

Cavina-Pratesi, Cristiana, Goodale, Melvyn A., Culham, Jody C., 2007. FMRI reveals a dissociation between grasping and perceiving the size of real 3D objects. PloS One 2 (5), e424.

Chaumon, Maximilien, DorothyBishop, VM, Niko, A. Busch, 2015. A practical guide to the selection of independent components of the electroencephalogram for artifact correction. J. Neurosci. Methods. 250, 47–63.

Culham, Jody C., Danckert, Stacey L., De Souza, Joseph F.X., Gati, Joseph S., Menon, Ravi S., Goodale, Melvyn A., 2003. Visually guided grasping produces fMRI activation in dorsal but not ventral stream brain areas. Experimental Brain Research. https://doi.org/10.1007/s00221-003-1591-5.

Donoghue, J.P., Sanes, J.N., Hatsopoulos, N.G., Gaál, G., 1998. Neural discharge and local field potential oscillations in primate motor cortex during voluntary movements. J. Neurophysiol. 79 (1), 159–173.

Fabbri, Sara, Stubbs, Kevin M., Cusack, Rhodri, Culham, Jody C., 2016. Disentangling representations of object and grasp properties in the human brain. J. Neurosci.: The Official Journal of the Society for Neuroscience 36 (29), 7648–7662.

Fagg, Andrew H., Arbib, Michael A., 1998. Modeling parietal-premotor interactions in primate control of grasping. Neural Network.: The Official Journal of the International Neural Network Society 11 (7–8), 1277–1303.

Goodale, M.A., Milner, A.D., Jakobson, L.S., Carey, D.P., 1991. A neurological dissociation between perceiving objects and grasping them. Nature. https://doi.org/10.1038/349154a0.

Grafton, S.T., Arbib, M.A., Fadiga, L., Rizzolatti, G., 1996. "Localization of grasp representations in humans by positron emission tomography. 2. Observation compared with imagination." experimental brain research. Experimentelle hirnforschung. Exp. Cereb. 112 (1), 103–111.

Guo, Lin Lawrence, Nestor, Adrian, Nemrodov, Dan, Frost, Adam, Niemeier, Matthias, 2019. Multivariate analysis of electrophysiological signals reveals the temporal properties of visuomotor computations for precision grips. J. Neurosci.: The Official Journal of the Society for Neuroscience 39 (48), 9585–9597.

Hazrati, Mehrnaz Kh, Erfanian, Abbas, 2010. "An online EEG-based brain–computer interface for controlling hand grasp using an adaptive probabilistic neural network. Medical Engineering & Physics. https://doi.org/10.1016/j.medengphy.2010.04.016.

Hebart, Martin N., Donner, Tobias H., Haynes, John-Dylan, 2012. Human visual and parietal cortex encode visual choices independent of motor plans. Neuroimage 63 (3), 1393–1403.

Himmelbach, Marc, Karnath, Hans-Otto, 2005. Dorsal and ventral stream interaction: contributions from optic ataxia. J. Cognit. Neurosci. https://doi.org/10.1162/0898929053467514.

Holm, Sture, 1980. On Multiple Test Procedures. Banach Center Publications. https://doi.org/10.4064/-6-1-159-168.

Iturrate, Iñaki, Chavarriaga, Ricardo, Pereira, Michael, Zhang, Huaijian, Corbet, Tiffany, Leeb, Robert, Millán, José Del R., 2018. Human EEG reveals distinct neural correlates of power and precision grasping types. Neuroimage 181 (November), 635–644.

Jarque-Bou, Néstor J., Margarita Vergara, Joaquín L. Sancho-Bru, Verónica gracia-ibáñez, Alba roda-Sales. 2019. "A Calibrated Database of Kinematics and EMG of the Forearm and Hand during Activities of Daily Living." Scientific Data. https://doi.org/10.1038/s41597-019-0285-1.

Jeannerod, M., Arbib, M.A., Rizzolatti, G., Sakata, H., 1995. Grasping objects: the cortical mechanisms of visuomotor transformation. Trends Neurosci. 18 (7), 314–320.

Jeannerod, M., Decety, J., Michel, F., 1994. Impairment of grasping movements following a bilateral posterior parietal lesion. Neuropsychologia 32 (4), 369–380.

Jiang, Tianxiao, Pellizzer, Giuseppe, Priscella Asman, Bastos, Dhiego, Bhavsar, Shreyas, Tummala, Sudhakar, Prabhu, Sujit, Nuri, F., Ince, 2020. Power modulations of ECoG alpha/beta and gamma bands correlate with time-derivative of force during hand grasp. Front. Neurosci. 14 (February), 100.

Jochumsen, Mads, Khan Niazi, Imran, Kim, Dremstrup, Ernest Nlandu Kamavuako, 2016. Detecting and classifying three different hand movement types through electroencephalography recordings for neurorehabilitation. Med. Biol. Eng. Comput. 54 (10), 1491–1501.

Klaes, Christian, Spencer, Kellis, Aflalo, Tyson, Lee, Brian, Pejsa, Kelsie, Shanfield, Kathleen, Hayes-Jackson, Stephanie, et al., 2015. Hand shape representations in the human posterior parietal cortex. J. Neurosci.: The Official Journal of the Society for Neuroscience 35 (46), 15466–15476.

Koehler, Saskia, Egetemeir, Johanna, Stenneken, Prisca, Koch, Stefan P., Paul, Pauli, Fallgatter, Andreas J., Herrmann, Martin J., 2012. The human execution/observation matching system investigated with a complex everyday task: a functional near-infrared spectroscopy (fNIRS) study. Neurosci. Lett. 508 (2), 73–77.

Koester, Dirk, Schack, Thomas, Jan, Westerholz, 2016. Neurophysiology of grasping actions: evidence from ERPs. Front. Psychol. 7 (December), 1996.

Kriegeskorte, Nikolaus, Mur, Marieke, Peter, Bandettini, 2008. Representational similarity analysis - connecting the branches of systems neuroscience. Front. Syst. Neurosci. 2 (November), 4.

Kruskal, Joseph, Wish, Myron, 1978. Multidimensional Scaling. https://doi.org/10.4135/9781412985130.

Michaels, Jonathan A., Scherberger, Hansjörg, 2018. Population coding of grasp and laterality-related information in the macaque fronto-parietal network. Sci. Rep. 8 (1), 1710.

Milner, A.D., Dijkerman, H.C., Pisella, L., McIntosh, R.D., Tilikete, C., Vighetto, A., Rossetti, Y., 2001. Grasping the past. Delay can improve visuomotor performance. Curr. Biol.: CB 11 (23), 1896–1901.

Mollazadeh, Mohsen, Aggarwal, Vikram, Singhal, Girish, Law, Andrew, Adam, Davidson, Schieber, Marc, Thakor, Nitish, 2008. "Spectral modulation of LFP activity in M1 during dexterous finger movements." *conference proceedings*, pp. 5314–5317. Annual International Conference of the IEEE Engineering in Medicine and Biology Society. IEEE Engineering in Medicine and Biology Society. Conference.

Muller-Putz, Gernot R., Rudiger Rupp, Patrick Ofner, Joana Pereira, Andreas Pinegger, Andreas Schwarz, Marcel Zube, Ute Eck, Bjorn Hessing, and Matthias Schneiders. 2019. "Applying intuitive EEG-controlled grasp neuroprostheses in individuals with spinal cord injury: preliminary results from the MoreGrasp clinical feasibility study." 2019 41st Annual International Conference of the IEEE Engineering in Medicine and Biology Society (EMBC). https://doi.org/10.1109/embc.2019.8856491.

Murata, A., Gallese, V., Luppino, G., Kaseda, M., Sakata, H., 2000. Selectivity for the shape, size, and orientation of objects for grasping in neurons of monkey parietal area AIP. J. Neurophysiol. 83 (5), 2580–2601.

Napier, J.R., 1956. "The prehensile movements of the human hand." *the Journal of Bone and joint surgery*. British 38-B (4), 902–913.

Ofner, Patrick, et al., 2019. Attempted arm and hand movements can be decoded from low-frequency EEG from persons with spinal cord injury. Scientific Reports 9 (1), 1–15.

Omedes, Jason, Schwarz, Andreas, Gernot, R., Müller-Putz, Montesano, Luis, 2018. Factors that affect error potentials during a grasping task: toward a hybrid natural movement decoding BCI. J. Neural. Eng. 15 (4), 046023.

Perini, Francesca, Powell, Thomas, Watt, Simon J., Downing, Paul E., 2020. Neural representations of haptic object size in the human brain revealed by multivoxel fMRI patterns. J. Neurophysiol. 124 (1), 218–231.

Pistohl, Tobias, Andreas, Schulze-Bonhage, Ad Aertsen, Carsten, Mehring, Tonio, Ball, 2012. Decoding natural grasp types from human ECoG. Neuroimage 59 (1), 248–260.

Polanen, Vonne van, Davare, Marco, 2015. Interactions between dorsal and ventral streams for controlling skilled grasp. Neuropsychologia. https://doi.org/10.1016/j.neuropsychologia.2015.07.010.

Rastogi, Anisha, Vargas-Irwin, Carlos E., Willett, Francis R., Abreu, Jessica, Crowder, Douglas C., Murphy, Brian A., Memberg, William D., et al., 2020a. Neural representation of observed, imagined, and attempted grasping force in motor cortex of individuals with chronic tetraplegia. Sci. Rep. 10 (1), 1429.

Rastogi, Anisha, Willett, Francis R., Abreu, Jessica, Crowder, Douglas C., Murphy, Brian A., Memberg, William D., Vargas-Irwin, Carlos E., et al., 2020b. The Neural Representation of Force across Grasp Types in Motor Cortex of Humans with Tetraplegia. https://doi.org/10.1101/2020.06.01.126755.

Rizzolatti, G., Fadiga, L., 1998. Grasping objects and grasping action meanings: the dual role of monkey rostroventral premotor cortex (area F5). Novartis Found. Symp. 218, 81–95 discussion 95–103.

Rizzolatti, G., Fadiga, L., Matelli, M., Bettinardi, V., Paulesu, E., Perani, D., Fazio, F., 1996. "Localization of grasp representations in humans by PET: 1. Observation versus execution." *experimental brain research. Experimentelle hirnforschung*. Exp. Cereb. 111 (2), 246–252.

Sburlea AI, Müller-Putz GR. n.d. "How similar are the neural patterns when observing grasping hand postures to the behavioral patterns when executing the grasp?" In Proceedings of the 8th Graz Brain-Computer Interface Conference 2019 Bridging Science and Application, edited by Gernot R. Müller-Putz, Jonas C. Ditz, Selina C. Wriessnegger, 279–84. Verlag der Technischen Universität Graz.

Sburlea, Andreea I., Müller-Putz, Gernot R., 2018. Exploring representations of human grasping in neural, muscle and kinematic signals. Sci. Rep. 8 (1), 16669.

Schaffelhofer, Stefan, Scherberger, Hansjörg, 2016. Object vision to hand action in macaque parietal, premotor, and motor cortices. eLife 5 (July). https://doi.org/10.7554/eLife.15278.

Schone, Hunter, R., et al., 2021. Expert tool users show increased differentiation between visual representations of hands and tools. J. Neurosci. 41 (13), 2980–2989.

Schwarz, Andreas, Ofner, Patrick, Pereira, Joana, , Andreea Ioana Sburlea, Gernot, R., Müller-Putz, 2018. Decoding natural reach-and-grasp actions from human EEG. J. Neural. Eng. 15 (1), 016005.

Smeets, J.B., Brenner, E., 1999. A new view on grasping. Mot. Contr. 3 (3), 237–271.

Su, L., Fonteneau, E., Marslen-Wilson, W., Kriegeskorte, N., 2012. Spatiotemporal searchlight representational similarity analysis in EMEG source space. Second International Workshop on Pattern Recognition in NeuroImaging. https://doi.org/10.1109/prni.2012.26.

Taniguchi, M., Kato, A., Fujita, N., Hirata, M., Tanaka, H., Kihara, T., Ninomiya, H., et al., 2000. Movement-related desynchronization of the cerebral cortex studied with spatially filtered magnetoencephalography. Neuroimage 12 (3), 298–306.

Turella, Luca, Lingnau, Angelika, 2014. Neural correlates of grasping. Front. Hum. Neurosci. 8 (September), 686.

Zaepffel, Manuel, Trachel, Romain, , Bjørg Elisabeth Kilavik, Brochier, Thomas, 2013. Modulations of EEG beta power during planning and execution of grasping movements. PloS One 8 (3), e60060.